

phys. stat. sol. (a) **63**, 229 (1981)

Subject classification: 1.4 and 14.4; 22.6.1

Laboratory of Inorganic Chemistry and Materials Science, Department of Chemical Engineering, Twente University of Technology, Enschede¹

Grain Boundary Effects on Ionic Conductivity in Ceramic $\text{Gd}_x\text{Zr}_{1-x}\text{O}_{2-(x/2)}$ Solid Solutions

By

T. VAN DIJK and A. J. BURGGRAAF

Complex admittance measurements are performed on high-purity ceramics prepared by means of the alkoxide synthesis and on less pure ceramics obtained from the citrate synthesis. The results on ceramic materials with grain sizes ranging from 0.4 to 20 μm are compared with those from a single crystal. The activation enthalpy for grain boundary conductivity $\Delta H_{\text{gb}} = (118 \pm 2)$ kJ/mol for the samples studied, is independent of composition, grain size, and preparation method. Grain boundary conductivity values and consequently the relevant pre-exponential factors are an order of magnitude smaller for the alkoxide materials than for the citrate materials. The ratio of grain bulk and grain boundary conductivity ($\sigma_{\text{b}}/\sigma_{\text{gb}}$) for alkoxide materials with grain-sizes 0.4 to 0.8 μm varies from 8.5 to 1.0 in the temperature range 500 to 700 °C.

Messungen der komplexen Admittanz werden an hochreinen keramischen Materialien, die mittels Alkoxidsynthese hergestellt wurden, und an weniger reinen Keramiken aus der Zitratsynthese gemessen. Die Ergebnisse an keramischen Materialien mit Korngrößen im Bereich von 0,4 bis 20 μm werden mit denen an einem Einkristall verglichen. Die Aktivierungsenthalpie für Korngrenzenleitfähigkeit beträgt $\Delta H_{\text{gb}} = (118 \pm 2)$ kJ/Mol für die untersuchten Proben, unabhängig von der Zusammensetzung, Korngröße und Präparationsmethode. Die Werte der Korngrenzenleitfähigkeit und dementsprechend die relevanten Präexponentialfaktoren sind für Alkoxid-Materialien eine Größenordnung geringer als für Zitratt-Materialien. Das Verhältnis der Kornvolumen- und Korngrenzenleitfähigkeit ($\sigma_{\text{b}}/\sigma_{\text{gb}}$) für Alkoxidmaterialien mit Korngrößen zwischen 0,4 und 0,8 μm variiert von 8,5 bis 1,0 im Temperaturbereich 500 bis 700 °C.

1. Introduction

The ionic conductivity of ceramic cubic stabilized zirconias depends on physical and chemical properties of the ceramic samples such as composition, ordering and ageing effects, porosity, grain size, and purity. Separation of grain bulk and grain boundary conductivity can be performed by complex plane analysis (see Section 3.1).

Ac conductivity investigations on $\text{ZrO}_2\text{-CaO}$ and $\text{ZrO}_2\text{-Y}_2\text{O}_3$ ceramics [1 to 7] revealed a large scatter in the grain boundary conductivity. The ratio of grain bulk and grain boundary conductivity at 500 °C, for example, varies from about 2.6 [3] to about 0.07 [4], although the same composition (0.91 $\text{ZrO}_2\text{-0.09 Y}_2\text{O}_3$) was studied. This ratio varies at 550 °C from 4.0 to 0.14 for 0.9 $\text{ZrO}_2\text{-0.1 Sc}_2\text{O}_3$ ceramic specimens with grain sizes 5 to 75 μm sintered at 1800 to 2200 °C during 4 h, but scatters between 0.5 and 0.2 for specimens with grain sizes 6 to 35 μm sintered at 2000 °C for 0.25 to 5.0 h [7]. This illustrates the influence of sample preparation conditions.

It appears that both grain bulk and grain boundary conductivities are decreased by adding impurities, frequently used as sintering aids [6, 8]. Mechanisms proposed to account for these effects are dissolution of impurities in the grains, segregation of them in the grain boundaries and, if present in higher concentrations, the formation of thin continuous or discontinuous layers of a second phase.

¹) P.O. Box 217, 7500 AE Enschede, The Netherlands.

Impurities of 1 mol% Fe_2O_3 , MgO , TiO_2 , and Al_2O_3 negatively influence the ionic conductivities of both the grains and the grain boundaries if compared with purer materials in the same study [6]. However, grain boundary conductivities of these very impure materials [6] far exceed those of samples containing only minor impurities [3]. A recent study on the influence of some mol% TiO_2 and Al_2O_3 as sintering aids in calcia-stabilized zirconia shows a strong deterioration of the performance of the impure materials compared with analytically or technically pure materials, even up to 1000 °C [8]. It seems likely that conflicting results obtained by various authors largely originate from preparation methods of the materials.

Analysis at 450 °C of grain boundary conductivity σ_{gb} as a function of grain size of yttria-stabilized zirconia prepared by means of the alkoxide synthesis [5] showed a linear increase of σ_{gb} with grain size for grain sizes larger than 4.5 μm . The variation of σ_{gb} with the grain size seems to be much less than linear for smaller grain sizes. However, the electrical behaviour of fine grain-sized ceramics has not yet been studied thoroughly. The grain bulk and grain boundary conductivity were found to have the same dependence on composition for $\text{Y}_x\text{Zr}_{1-x}\text{O}_{2-(x/2)}$ solid solutions [4].

In all investigations [1 to 7] the activation enthalpy for grain boundary conductivity was found to be higher than that of grain bulk conductivity.

The aim of this paper is to compare the grain boundary conductivities of ceramic samples with both small grain sizes and well defined microstructures and purity levels. In addition values of the activation enthalpy and pre-exponential factor for grain boundary conductivity are compared with corresponding quantities for grain bulk-conductivities. Studies on grain boundaries, achieved by intergranular breaking techniques, have been started on selected suitable specimens.

Samples with different purity levels were obtained from either the alkoxide or the citrate synthesis. Variation of the grain size of the samples was achieved by varying the sintering temperature.

2. Experimental Procedures

2.1 Specimen preparation and characterization

In this investigation $\text{Gd}_x\text{Zr}_{1-x}\text{O}_{2-(x/2)}$ solid solutions were studied from one of three following different preparation methods:

- i) single crystals, grown from a skull-melting procedure [9],
- ii) dense ultrafine grain ceramics resulting from the "alkoxide synthesis" [10, 11],
- iii) dense fine-grain ceramics obtained from the "citrate synthesis".

Each of the two wet-chemical preparation methods results in sinter-reactive powders from which at relatively low temperatures dense ceramic samples can be obtained having their own characteristics with respect to grain size, purity, etc.

The polycrystalline specimens were characterized by X-ray diffraction, X-ray fluorescence analysis of the chemical composition, pycnometric determination of the density, and determination of the grain sizes of the samples by means of scanning electron microscopy. Grain size was measured by the Mendelssohn line intersection method and occasionally by the estimation of the grain size distribution using a correction method described by Oel [12].

All ceramic samples were disc-shaped. The single crystalline specimen was plate-like with dimensions of about $1 \times 3 \times 7 \text{ mm}^3$. Pt electrodes with thicknesses of about 2 μm were sputtered onto opposite surfaces of the samples.

Ac conductivity measurements in the frequency range 10^2 to 10^7 Hz were performed in the temperature range 500 to 750 °C using a Hewlett Packard network analyser 3570 A in combination with an automatic synthesizer HP 3330B.

2.1.1 Single crystalline material²⁾

A sample with composition $\text{Gd}_{0.52}\text{Zr}_{0.48}\text{O}_{1.74}$ was prepared by the method described in [9].

After annealing at 1250 °C during 200 h the material has the cubic fluorite-related pyrochlore structure. The influence of ordering on the conductivity of this material was described in a previous paper [13].

The ac conductivity of the single crystalline material is presented here to show the difference between the ac conductivity behaviour of single crystalline and polycrystalline material and to justify the validity of the equivalent electrical circuit used to separate grain bulk and grain boundary conductivity.

2.1.2 Alkoxide material

Fine-grained ceramics with composition $\text{Gd}_{0.495}\text{Zr}_{0.505}\text{O}_{1.753}$ were prepared from alkoxide powders [10, 11].

Alkoxide powder preparation was performed by hydrolysis of a metal alkoxide mixture. The metal alkoxides used were Zr-*t*-amyl oxide $\text{Zr}(\text{OC}_5\text{H}_{11})_4$ and Gd-iso-propoxide $\text{Gd}(\text{OC}_3\text{H}_7)_3$. A diluted metal alkoxide-benzene solution was added dropwise to a large excess of water while vigorously stirring.

Subsequently the precipitated hydroxide was rinsed with water three times and in addition intensively washed with isopropanol in order to remove the water. After drying, the powders were dry-milled for a short period in a teflon ball-mill, calcinated at 650 °C and dry-milled again. Finally the material was isostatically pressed at 400 MPa and sintered in oxygen at temperatures of 1400 or 1430 °C during 5 h.

2.1.3 Citrate material

Samples with various compositions were prepared by the wetchemical citrate method [14] based upon a procedure first proposed by Marcilly [15]. Grain size variation was achieved by sintering the samples either at 1550 °C during 70 h or at 1700 °C during 20 h.

3. Grain Boundary Effects and the Equivalent Electrical Circuit

3.1 Ac conductivity behaviour

Compared with single crystalline material, ceramic samples consist of grains with a high conductivity, separated by relatively thin grain boundaries. Oxygen conducting ceramics, developed up to now, always exhibit smaller specific conductivity than the individual (single crystalline) grains. Geometrically a parallel conduction path along

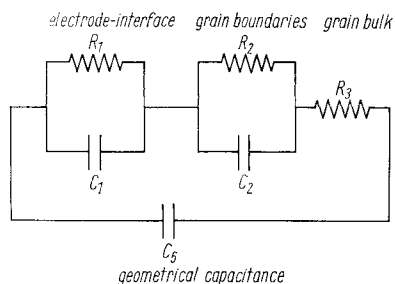


Fig. 1. Electrical equivalent circuit of a ceramic sample with electrodes. R_1 — resistance of the electrode interface, C_1 — capacitance of the electrode interface, R_2 — resistance of the grain boundaries, C_2 — capacitance of the grain boundaries, R_3 — resistance of the grains, C — geometrical capacitance

²⁾ The single-crystalline material was kindly placed at our disposal by Dr. M. Perez y Jorba, CNRS, Vitry, France.

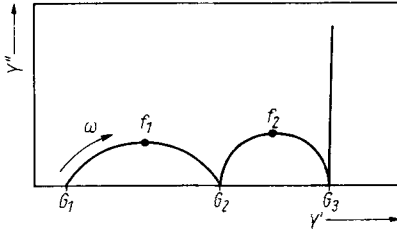


Fig. 2. Complex admittance diagram representing the electrical equivalent circuit of Fig. 1.

$$G_1 = \frac{1}{R_1 + R_2 + R_3}, \quad G_2 = \frac{1}{R_2 + R_3}, \quad G_3 = \frac{1}{R_3}, \quad C_1 = \frac{G_2^2}{2\pi f_1(G_2 - G_1)}, \quad C_2 = \frac{G_3^2}{2\pi f_2(G_3 - G_2)},$$

the grain boundaries is not likely if it is assumed that the specific “microscopic” conductivity of the grain boundaries is smaller than the bulk conductivity.

If in addition to this the electrode interface and the geometrical capacitance are taken into account, the relatively simple equivalent electrical circuit representing the polycrystalline sample with electrodes is depicted in Fig. 1. It was developed originally by Bauerle [1].

Although this equivalent circuit is frequently used in literature, its correctness should be justified by comparing results obtained from single crystalline and polycrystalline materials. The approximation of the electrical properties of the sample by the equivalent electrical circuit representation of Fig. 1 strongly depends on uniform grain bulk and grain boundary properties over the entire specimen. This has recently been discussed by de Jonghe [16] with regard to sodium beta alumina.

As the relaxation times associated with grain boundary polarizations, electrode interface polarizations and geometrical capacitance are different, the equivalent circuit can be analysed by ac frequency dispersion techniques.

The complete complex admittance diagram associated with the equivalent scheme of Fig. 1 is depicted in Fig. 2 where it is also shown how conductivity and capacity values can be determined from the intercepts of the semicircles with the horizontal axis and the frequency values at the semicircle maxima.

3.2 Microscopic interpretation of macroscopic grain boundary conductivity and capacitance data

3.2.1 The specific conductivity of the grain boundaries

Generally the macroscopic conductivity $\sigma_{gb}^{(mac)} = (1/R_2)(L/A)$ (L/A is the length-area ratio of the sample) of the grain boundaries can be obtained from the complex admittance plots. To characterize the grain boundaries it is possible, with certain assumptions, to obtain at least an order of magnitude estimation of the “microscopic” conductivity associated with the grain boundaries.

The grains are assumed to be cube-shaped with edges d_g and separated by grain boundaries with thickness δ_{gb} . In this phenomenological description it is immaterial whether the grain boundaries are “intrinsic” due to segregation effects and grain boundary space charge or “extrinsic” due to second phase formation at the boundaries [17, 18].

If the “microscopic” conductivity of the grain boundaries is $\sigma_{gb}^{(mic)}$ it follows for the conductance:

$$\frac{1}{R_2} = \sigma_{gb}^{(mic)} \frac{A}{\delta_{gb}} \frac{(d_g + \delta_{gb})}{L}, \quad (1)$$

where $L/(d_g + \delta_{gb}) \approx L/d_g$ represents the number of grain boundaries in the direction of the electric field.

From equation (1) it follows for the relation of “microscopic” and “macroscopic” grain boundary conductivity ($1/R_2$) (L/A)

$$\sigma_{gb}^{(\text{mic})} = \sigma_{gb}^{(\text{mac})} \frac{\delta_{gb}}{d_g}. \quad (2)$$

It appears that for grain sizes larger than $1 \mu\text{m}$ the microscopic grain boundary conductivity is several orders of magnitude smaller than the macroscopic one because the intrinsic grain boundary thickness is usually of the order 1 to 10 nm [17, 18].

From (2) it follows that enhancement of the macroscopic grain boundary conductivity can be performed by grain growth, narrower grain boundaries, or optimizing microscopic specific grain boundary conductivity.

It is generally stated [1, 4] that it is essentially the non-zero impurity concentration at the grain boundaries which has a large influence on the low grain boundary conductivity. Unfortunately very few data are available in literature for evaluating the influence of grain boundary segregation in contrast to second phase formation.

3.2.2 Capacity and dielectric constant associated with grain boundaries

Using the same simple model as in the preceding section, the quantity C_2 (L/A) can be correlated with the dielectric constant associated with the grain boundaries.

It follows that for each grain boundary intersection C_i perpendicular to the electric field

$$C_i = \varepsilon_0 \varepsilon_{r_{gb}} \frac{A}{\delta_{gb}}. \quad (3)$$

For all $L/(d_g + \delta_{gb}) \approx L/d_g$ intersections it follows that

$$\frac{1}{C_2} = \frac{L}{d_g} \frac{1}{C_i}. \quad (4)$$

or combining (3) and (4)

$$C_2 \frac{L}{A} = \varepsilon_0 \varepsilon_{r_{gb}} \frac{d_g}{\delta_{gb}}. \quad (5)$$

The importance of (5) is that, assuming a reasonable value for $\varepsilon_{r_{gb}}$, from the capacity obtained from the maximum of the grain boundary semicircle a reasonable value for δ_{gb} can be found.

4. Results and Discussion

4.1 Characterization of specimens

Samples prepared by means of the alkoxide synthesis and sintered at 1400 to 1430 °C appear to have ceramic microstructures which compare well with those of citrate materials, sintered at 1550 °C.

The main difference is the impurity level of both samples (see Table 1). The citrate materials contain about ten times as many impurities as the alkoxide materials, the main impurities being SiO_2 and Al_2O_3 .

The microstructures of the materials investigated are well developed with only few isolated pores on the grain boundaries, the remaining pores being located in the grains. Some of the grain boundaries are irregularly curved indicating that grain growth has not completely stopped and grain boundaries exist in a non-equilibrium state. Typical micrographs of alkoxide and citrate materials are shown in Fig. 3.

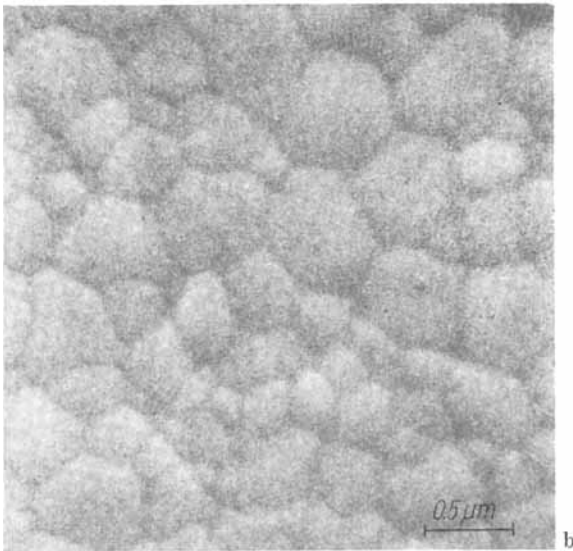
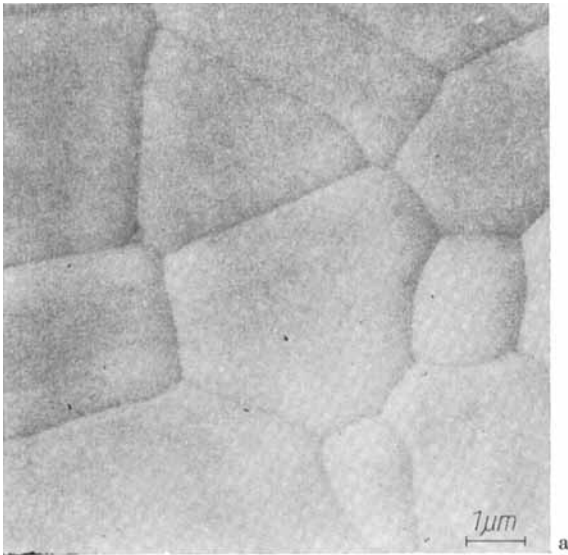


Fig. 3. a) SEM micrograph of $\text{Gd}_{0.498}\text{Zr}_{0.502}\text{O}_{1.751}$ sintered at 1700 °C (citrate synthesis); b) SEM micrograph of $\text{Gd}_{0.495}\text{Zr}_{0.505}\text{O}_{1.752}$ sintered at 1400 °C (alkoxide synthesis)

The grain size distributions, corrected according to Oel [12] were measured for the citrate materials with composition 49.8 mol% $\text{GdO}_{1.5}$ (see Fig. 4 for the grain size distribution of the sample, sintered at 1700 °C).

Mean grain sizes of the materials and relevant standard deviations of the distributions are contained in Table 3.

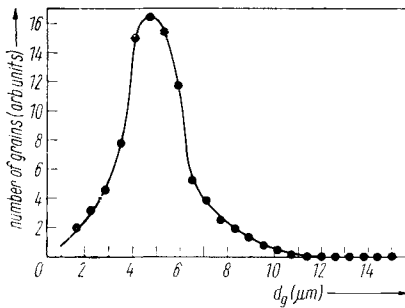


Fig. 4. Grain size distribution of $\text{Gd}_{0.498}\text{O}_{0.502}\text{O}_{17.51}$ (citrate synthesis) sintered at 1700°C corrected after Oel [12]

Table 1
Impurities of alkoxide and citrate materials

type of synthesis	$\text{GdO}_{1.5}$ (at%)	SiO_2 (wt%)	Al_2O_3 (wt%)	C (wt%)	Fe (wt%)
alkoxide	49.5	7×10^{-3}	$<4 \times 10^{-2}$ *	—	—
citrate	44.8/49.8/53.2	0.1 to 0.15	0.1	0.03	0.01

*) Detection limit.

4.2 Complex admittance measurements

4.2.1 Validity of the electrical equivalent circuit

Complex admittance plots at 500°C are shown in Fig. 5 for ceramic alkoxide, citrate, and single crystalline samples with compositions 49.5, 49.8, and 52 mol% $\text{GdO}_{1.5}$, respectively. A semicircle is found for both types of ceramic materials in the frequency range 10^4 to 10^6 Hz. The diameter of this semicircle depends on grain size (Fig. 5).

Apparently this semicircle is absent for the single crystalline sample (Fig. 5c) where only relaxation phenomena having their maxima at frequencies $< 10^2$ Hz and $> 10^6$ Hz are observed. These can be attributed to electrode interface polarization phenomena and the geometrical capacitance of the sample, respectively. This indicates that the polarization phenomena observed for the ceramic samples are due to the ceramic microstructures of the samples, essentially the presence of grain boundaries. From Fig. 5a and b it is evident that the grain boundary dispersion is much larger for the alkoxide than for the citrate material.

For both types of ceramic materials the centres of the semicircles are located only slightly below the horizontal σ' -axis. This probably indicates uniform grain boundary properties throughout the samples, whereas a wide distribution of these properties causes a large dispersion in relaxation times and consequently makes the semicircle centre fall below the horizontal axis [1, 16].

The availability of two types of ceramic materials with approximately the same composition exhibiting apparently widely differing grain boundary properties, as well as single crystalline material, enables us to demonstrate both the justification of the electrical equivalent circuit (Fig. 1) and the independence of grain bulk conductivity (the high frequency intercept of the grain boundary polarization semicircle with the horizontal axis) on microstructure.

From Table 2 it follows that the bulk conductivity of materials with identical compositions is, within experimental error, independent of material preparation.

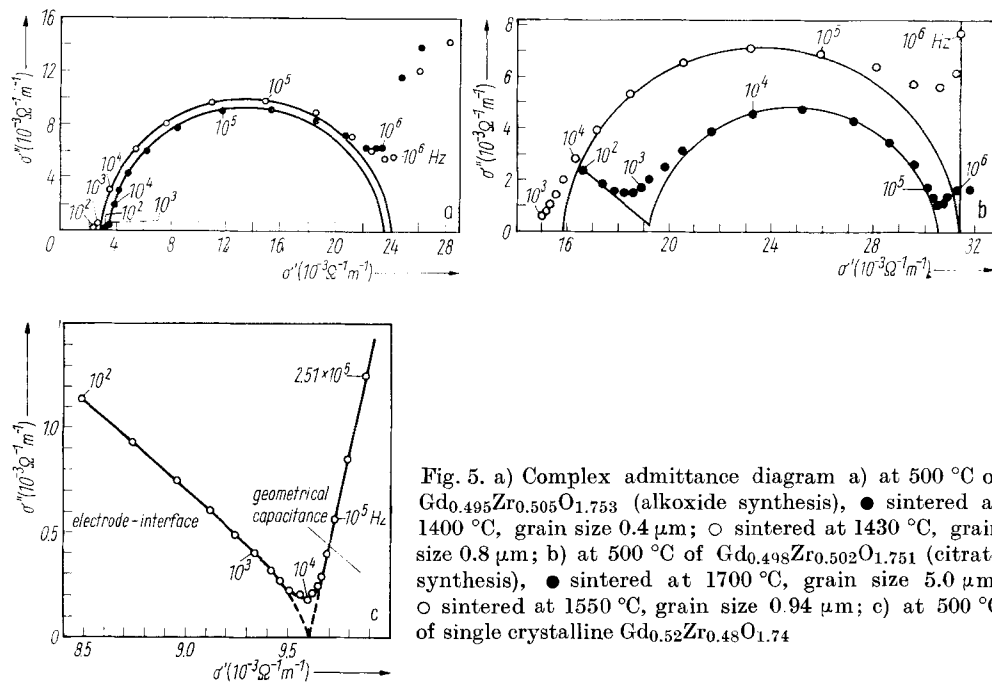


Fig. 5. a) Complex admittance diagram a) at 500 °C of $\text{Gd}_{0.495}\text{Zr}_{0.505}\text{O}_{1.753}$ (alkoxide synthesis), ● sintered at 1400 °C, grain size 0.4 μm ; ○ sintered at 1430 °C, grain size 0.8 μm ; b) at 500 °C of $\text{Gd}_{0.498}\text{Zr}_{0.502}\text{O}_{1.751}$ (citrate synthesis), ● sintered at 1700 °C, grain size 5.0 μm , ○ sintered at 1550 °C, grain size 0.94 μm ; c) at 500 °C of single crystalline $\text{Gd}_{0.52}\text{Zr}_{0.48}\text{O}_{1.74}$

Conductivity values of the single crystalline material coincide with values obtained from previous ceramic data [13].

Table 2

Comparison of bulk conductivity values for citrate, alkoxide, and single crystalline (SC) materials

GdO _{1.5} (mol%)	method	phase	bulk ionic conductivity ($10^{-3}(\Omega\text{m})^{-1}$)		
			500 °C	600 °C	700 °C
44.8	citrate	F	4.1	28	102
49.5	alkoxide	P	24	110	267
49.8	citrate	P	31	140	345
52	SC	P	9.5	52	173
52	citrate [13]	P	9.0	44	150
53.2	citrate	P	4.1	25	95

4.2.2 The grain boundary conductivity of alkoxide and citrate material

Grain boundary conductivities of several samples prepared by means of the citrate and alkoxide synthesis are plotted as a function of temperature in Fig. 6 together with results of Schouler et al. [3] for 0.91 ZrO_2 -0.09 Y_2O_3 and of Chu and Seitz [2] for 0.05 ZrO_2 -0.15 CaO .

It appears from Fig. 6 that the grain boundary conductivities of the citrate materials exceed those of the alkoxide materials by more than one order of magnitude. Besides

this it appears that the grain boundary conductivities of the citrate samples are larger and those of the alkoxide samples are smaller than the literature values mentioned for structurally related systems (however with a strongly different lanthanide concentration).

For temperatures above 650 °C, grain boundary conductivities of citrate materials seem to increase faster with increasing temperature than is to be expected from the Arrhenius behaviour below 650 °C. However, as the semicircles are very small and bulk conductivities are relatively high at higher temperatures, large errors are involved in estimating the grain boundary conductivities at temperatures higher than 650 °C.

The ratios of grain bulk and grain boundary conductivity of some samples are shown as a function of temperature in Fig. 7. In the temperature range measured, σ_b was in all cases larger than σ_{gb} for the alkoxide material and practically always smaller than σ_{gb} for the citrate material. This cannot be explained by differences in grain size (cf. Δ and \blacksquare in Fig. 7). σ_b/σ_{gb} values were found for alkoxide materials at 500 °C which were larger than those reported in literature [1 to 7] and which range from about 4 to 0.1. The bends in the curves of Fig. 7 arise at least partially from the grain bulk conductivity behaviour, because in the temperature range investigated a bend in the $\log \sigma_b$ versus $1/T$ curve is often observed for stabilized zirconias.

From Fig. 6 and 7 it appears that the grain boundary conductivity depends strongly on material preparation and/or purity.

Surprisingly, the smaller grain size alkoxide sample has a larger σ_{gb} than the larger grain size alkoxide. The difference is, however, too small to be conclusive. More detailed studies of this grain size range, taking into account grain size distributions are at present under investigation.

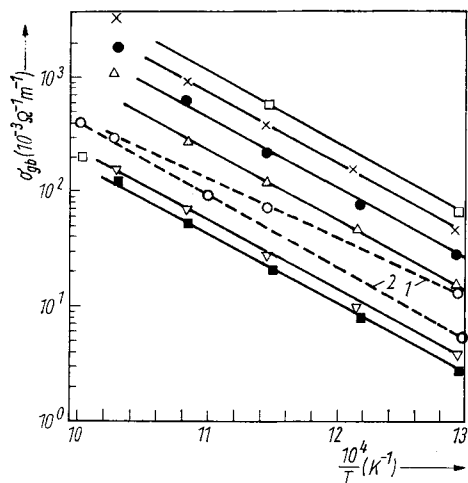


Fig. 6

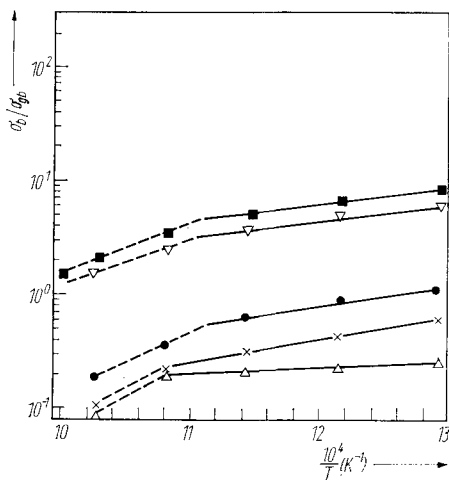


Fig. 7

Fig. 6. Arrhenius plots of grain boundary conductivity of various citrate and alkoxide samples. \times $Gd_{0.498}Zr_{0.502}O_{1.751}$ (citrate synthesis) sintered at 1700 °C, grain size 5 μm ; \circ $Gd_{0.498}Zr_{0.502}O_{1.751}$ (citrate synthesis) sintered at 1550 °C, grain size 0.94 μm ; Δ $Gd_{0.448}Zr_{0.552}O_{1.776}$ (citrate synthesis) sintered at 1550 °C, grain size 0.8 μm ; \square $Gd_{0.532}Zr_{0.467}O_{1.734}$ (citrate synthesis) sintered at 1700 °C, grain size 20 μm ; ∇ $Gd_{0.495}Zr_{0.505}O_{1.753}$ (alkoxide synthesis), sintered at 1400 °C, grain size 0.4 μm ; \blacksquare $Gd_{0.495}Zr_{0.505}O_{1.753}$ (alkoxide synthesis), sintered at 1430 °C, grain size 0.8 μm

Fig. 7. Ratio of grain bulk σ_b and grain boundary conductivity σ_{gb} as a function of temperature (symbols see Fig. 6)

The values of the activation enthalpy ΔH and the pre-exponential factor σ_0 for grain bulk and grain boundary conductivity obtained from Arrhenius plots are shown in Table 3.

Table 3

Activation enthalpy and pre-exponential factors for grain bulk and grain boundary conductivity for citrate, alkoxide, and single crystalline materials

GdO _{1.5} (mol%)	prepara- tion method	T_s (°C)	d_g (μm)	$\varrho/\varrho_{\text{th}}$ (%)	ΔH_b (kJ/mol)	σ_{0b} ($10^3 (\Omega \text{ m})^{-1}$)	ΔH_{gb} (kJ/mol)	$\sigma_{0gb}^{(\text{mac})}$ ($10^6 (\Omega \text{ m})^{-1}$)
44.8	C	1550	0.8	98	107.3	70.2	116.8	1.22
49.8	C	1550	0.94 (0.35)	96	79.8	7.9	117.5	2.4
49.8	C	1700	5.0 (2.0)	98.5	79.8	7.9	118.1	4.6
53.2	C	1700	20	95	99.6	21.0	119.6	8.6
49.5	A	1400	0.4	93	80.2	5.6	116.5	0.28
49.5	A	1430	0.8	94	80.2	5.6	120.2	0.36
52	S(CP-Phase)	—	—	—	97.2	34.2	—	—

The independence of material preparation for ΔH_b and σ_{0b} is again illustrated together with the minimum values for ΔH_b and σ_{0b} in the stoichiometric pyrochlore phase with 50 at% GdO_{1.5} as was reported earlier [13].

The large compositional effect on ΔH_b and σ_{0b} is not observed for ΔH_{gb} and σ_{0gb} .

ΔH_{gb} is always larger than ΔH_b and in fact for both citrate and alkoxide samples the $\Delta H_{gb} = (118 \pm 2)$ kJ/mol, independent of composition, grain size, and preparation method.

The values for σ_{0gb} for the citrate materials are all in the range 1 to $10 \times 10^6 (\Omega \text{ m})^{-1}$. Neither a pronounced compositional behaviour as for σ_{0b} nor a linear relation with grain size seems to exist.

The values of σ_{0gb} of the citrate materials mutually differ much less than they do from the values for alkoxide materials. It is also seen from Table 3 that the larger grain size alkoxide sample has the larger σ_{0gb} (cf. Fig. 5 and 7).

It is now obvious from Table 3 that low grain boundary conductivities occur at relatively low temperatures due to the high activation enthalpy for grain boundary

Table 4

Microscopic and macroscopic σ_{0b} values for citrate and alkoxide materials

GdO _{1.5} (at%)	preparation method	grain size (μm)	macroscopic	microscopic	
			σ_{0gb} ($10^6 (\Omega \text{ m})^{-1}$)	I. $\delta_{gb} = 1 \text{ nm}$ σ_{0gb} ($10^2 (\Omega \text{ m})^{-1}$)	II. $\delta_{gb} = 10 \text{ nm}$ σ_{0gb} ($10^3 (\Omega \text{ m})^{-1}$)
44.8	C	0.8	1.2	15	15
49.8	C	0.94	2.4	26	26
49.8	C	5.0	4.6	9	9
53.2	C	20	8.6	4	4
49.5	A	0.4	0.28	7	7
49.5	A	0.8	0.36	4.5	4.5

conductivity. The contribution of grain boundaries to the total resistivity of the sample becomes negligible at high temperatures due to the macroscopic $\sigma_{0_{\text{gb}}}^{(\text{mac})}$ values which are large compared with the $\sigma_{0_{\text{b}}}$ values.

Microscopic $\sigma_{0_{\text{gb}}}^{(\text{mic})}$ values derived from the macroscopic ones tabulated in Table 3 which were obtained by multiplication of $\sigma_{0_{\text{b}}}^{(\text{mac})}$ with $\delta_{\text{gb}}/d_{\text{g}}$ are shown in Table 4.

A reasonable choice has to be made for the unknown boundary thickness δ_{gb} . As extreme values in cases I and II, $\delta = 1$ nm and 10 nm were taken [17, 18].

Of course values in Table 4 have to be interpreted with care. However, it seems likely from a comparison of Tables 3 and 4 that with the possible exception of the samples with about 50 mol% $\text{GdO}_{1.5}$, where $\sigma_{0_{\text{b}}}$ is minimum [13], microscopic $\sigma_{0_{\text{gb}}}^{(\text{mic})}$ values are at least half an order of magnitude smaller than $\sigma_{0_{\text{b}}}$ values. Due to the influence of ΔH_{gb} the microscopic $\sigma_{\text{gb}}^{(\text{mic})}$ is always much smaller than the conductivity of the grains.

In conclusion it thus appears that the activation enthalpy for grain boundary conductivity is independent of bulk composition and materials preparation. In addition very pure alkoxide material has a smaller pre-exponential factor for grain boundary conductivity than the less pure citrate material.

The constant activation enthalpy cannot be easily explained by segregation of one of the main components (Gd^{3+} or Zr^{4+}) in the grain boundary regions as this would involve (i) large differences in composition between bulk and grain boundary regions³⁾ or (ii) an overall concentration independent segregation effect which is theoretically not very likely [17, 18].

However, the formation of a thin relatively isolating film of impurity material on the grain boundaries cannot be completely ignored although this is at least more likely in citrate materials because of their higher impurity level compared with alkoxide material.

From literature [17, 18] it is known that space charges are likely to exist at the grain boundaries of ceramics with thicknesses of about 1 to 10 nm. If an electric field is applied to the specimen, another space charge is induced at the grain boundaries due to the difference in specific conductivity of bulk and grain boundary material [19].

Possibly the constant ΔH_{gb} occurs because a predominant energy term in this activation enthalpy is the energy required to transfer the mobile species from the bulk into the grain boundary space charge region.

Table 5

The capacitance at 500 °C of the grain boundaries and the corresponding calculated δ_{gb} ($\epsilon_r = 70$)

composition $\text{GdO}_{1.5}$ (at%)	method	T_{g} (°C)	grain size (μm)	C_2 (L/A) (nFm^{-1})	δ_{gb} (calc) (nm)
44.8	C	1550	0.8	186	2.7
49.8	C	1550	0.94	153	3.8
49.8	C	1700	5.0	631	4.9
53.2	C	1700	20	5876	2.1
49.5	A	1400	0.4	39.4	6.3
49.5	A	1430	0.8	74.2	6.7

³⁾ In the case of the sample with 49.8 mol% $\text{GdO}_{1.5}$ the grain boundary composition should be approximately 40 mol% $\text{GdO}_{1.5}$ in order to yield the experimentally observed ΔH_{gb} .

If impurities are present in such amounts that they constrict grain boundaries by the formation of an electrically isolating second phase or a thin film around the grains, their negative effect on grain boundary conductivity is evident. However, this is not observed in citrate materials.

4.2.3 The grain boundary capacitance

The grain boundary capacitances $C_2(L/A)$ obtained from the maxima of the grain boundary polarization semicircles at 500 °C are listed in Table 5.

Also the δ_{gb} values which can be calculated from (5) (Section 3.2.2) are shown.

As a reasonable value for the dielectric constant of the grain boundaries the single crystal value ($\epsilon_r = 70$) was taken. It is seen from Table 5 that the variation of $C_2(L/A)$ with grain size is roughly linear.

Calculated values for δ_{gb} are then all in the range of a few nm. Such values for the grain boundary thicknesses were described in literature [17, 18]. In addition the calculation of $\sigma_{0gb}^{(mic)}$ from $\sigma_{0gb}^{(mac)}$ in Section 2.2 assuming values for δ_{gb} between 1 and 10 nm seems reasonable.

Acknowledgements

The authors would like to thank Dr. K. J. de Vries for assisting with electrical measurements, Mr. M. A. C. G. van de Graaf for supplying the alkoxide materials, and Mr. H. Kruidhof for chemical analysis of the samples.

References

- [1] J. E. BAUERLE, *J. Phys. Chem. Solids* **30**, 2657 (1969).
- [2] S. H. CHU and M. A. SEITZ, *J. Solid State Chem.* **23**, 297 (1978).
- [3] E. SCHOULER, G. GIROUD, and M. KLEITZ, *J. Chim. phys. et Physico-chim. biol.* **70**, 1309 (1973).
- [4] M. V. INOZEMTSEV and M. V. PERFILEV, *Elektrokhimiya* **12**, 1236 (1976).
- [5] A. I. IOFFE, M. V. INOZEMTSEV, A. S. LIPILIN, M. V. PERFILEV, and S. V. KARPACHOV, *phys. stat. sol. (a)* **30**, 87 (1975).
- [6] M. V. INOZEMTSEV and M. V. PERFILEV, *Elektrokhimiya* **11**, 1031 (1975).
- [7] M. V. INOZEMTSEV, M. V. PERFILEV, and A. S. LIPILIN, *Elektrokhimiya* **10**, 1471 (1974).
- [8] K. C. RADFORD and R. J. BRATTON, *J. Mater. Sci.* **14**, 66 (1979).
- [9] M. PEREZ Y JORBA and R. COLLONGUES, *Rev. Internat. Hautes Temp. Refract.* **1**, 21 (1964).
- [10] K. S. MAZDIYASNI, C. T. LYNCH, and J. S. SMITH II, *J. Amer. Ceram. Soc.* **50**, 532 (1967).
- [11] M. A. C. G. VAN DE GRAAF, K. KEIZER, and A. J. BURGGRAAF, *Science of Ceramics*, Vol. 10, De Nederlandse Keramische Vereniging, Enschede 1980 (in the press).
- [12] H. J. OEL, *Ber. Dtsch. Keram. Ges.* **43**, 624 (1966).
- [13] T. VAN DIJK, K. J. DE VRIES, and A. J. BURGGRAAF, *phys. stat. sol. (a)* **58**, 115 (1980).
- [14] M. A. C. G. VAN DE GRAAF, T. VAN DIJK, K. J. DE VRIES, and A. J. BURGGRAAF, *Science of Ceramics*, Vol. 9, Ed. K. J. DE VRIES, De Nederlandse Keramische Vereniging, Enschede 1977 (p. 75).
- [15] C. MARCILLY, Thesis, Université de Grenoble, 1968.
- [16] L. C. DE JONGHE, *J. Mater. Sci.* **14**, 33 (1979).
- [17] W. D. KINGERY, *J. Amer. Ceram. Soc.* **57**, 1 (1974).
- [18] W. D. KINGERY, *J. Amer. Ceram. Soc.* **57**, 74 (1974).
- [19] W. D. KINGERY, H. K. BOWEN, and D. R. UHLMANN, *Introduction to Ceramics* Chap. 18, John Wiley and Sons, New York 1976.

(Received July 25, 1980)